

Radiation Effect On Unsteady MHD Free Convective Flow Past An Exponentially Accelerated Vertical Plate With Viscous And Joule Dissipations

Maitree Jana¹, Sanatan Das² and Rabindra Nath Jana³

^{1,3}(Department of Applied Mathematics, Vidyasagar University, Midnapore 721 102, India)

²(Department of Mathematics, University of Gour Banga, Malda 732 103, India)

ABSTRACT

The effects of radiation on unsteady MHD free convection flow of a viscous incompressible electrically conducting fluid past an exponentially accelerated vertical plate in the presence of a uniform transverse magnetic field on taking viscous and Joule dissipations into account have been studied. The governing equations have been solved numerically by the implicit finite difference method of Crank- Nicolson's type. The variations of velocity and fluid temperature are presented graphically. It is found that both the magnetic field and radiation decelerate the fluid velocity. An increase in Eckert number leads to rise in fluid velocity and temperature. Further, it is found that the magnitude of the shear stress at the plate increases with an increase in either radiation parameter or magnetic parameter. The rate of heat transfer at the plate decreases with an increase in radiation parameter.

Keywords: MHD free convection, radiative heat transfer, Prandtl number and Grashof number, viscous and Joule dissipations.

I. INTRODUCTION

The most common type of body force on a fluid is gravity defined in magnitude and direction by the corresponding acceleration vector. Sometimes, electromagnetic effects are important. The electric and magnetic fields themselves obey a set of physical laws, which are expressed by Maxwell's equations. The solution of such problems requires the simultaneous solution of the equations of fluid mechanics and of electromagnetism. One special case of this type of coupling is the field known as magnetohydrodynamics (MHD). The hydromagnetic flows and heat transfer have become more important in recent years because of its varied applications in agricultural engineering and petroleum industries. Recently, considerable attention has also been focused on new applications of magnetohydrodynamics (MHD) and heat transfer such as metallurgical processing. Melt refining involves magnetic field applications to control excessive heat transfer rate. Other applications of MHD heat transfer include MHD generators, plasma

propulsion in astronautics, nuclear reactor thermal dynamics and ionized-geothermal energy systems.

An excellent summary of applications can be found in Hughes and Young [1]. Abd-El-Naby et al.[2] have studied the finite difference solution of radiation effects on MHD free convection flow over a vertical plate with variable surface temperature. The transient radiative hydromagnetic free convection flow past an impulsively started vertical plate with uniform heat and mass flux have been investigated by Ramachandra Prasad et al. [3]. Takhar et al.[4] have analyzed the radiation effects on MHD free convection flow of a radiating fluid past a semi-infinite vertical plate using Runge-Kutta-Merson quadrature. Samria et al. [5] studied the hydromagnetic free convection laminar flow of an elasto-viscous fluid past an infinite plate. Recently, the natural convection flow of a conducting visco-elastic liquid between two heated vertical plates under the influence of transverse magnetic field has been studied by Sreehari Reddy et al.[6]. In all these investigations, the viscous dissipation is neglected. The viscous dissipation heat in the natural convective flow is important, when the flow field is of extreme size or at low temperature or in high gravitational field. Such effects are also important in geophysical flows and also in certain industrial operations and are usually characterized by the Eckert number. A number of authors have considered viscous heating effects on Newtonian flows. Maharajan and Gebhart [7] reported the influence of viscous dissipation effects in natural convective flows, showing that the heat transfer rates are reduced by an increase in the dissipation parameter. Israel-Cookey et al. [8] have investigated the influence of viscous dissipation and radiation on unsteady MHD free convection flow past an infinite heated vertical plate in a porous medium with time dependent suction. Zueco Jordan [9] has used network simulation method (NSM) to study the effects of viscous dissipation and radiation on unsteady MHD free convection flow past a vertical porous plate. Suneetha et al. [10] have analyzed the effects of viscous dissipation and thermal radiation on hydromagnetic free convection flow past an impulsively started vertical plate. Suneetha et al.[11]

have studied the effects of thermal radiation on the natural convective heat and mass transfer of a viscous incompressible gray absorbing-emitting fluid flowing past an impulsively started moving vertical plate with viscous dissipation. Ahmed and Batin [12] have obtained an analytical model of MHD mixed convective radiating fluid with viscous dissipative heat.

The objective of the present work is to study the effects of radiation on unsteady MHD free convective flow of a viscous incompressible electrically conducting fluid past an exponentially accelerated vertical plate in the presence of a uniform transverse magnetic field on taking viscous and Joule dissipations into account. At time $t \leq 0$, both the fluid and plate are at rest with constant temperature T_∞ . At time $t > 0$, the plate at $y = 0$ starts to move in its own plane with a velocity $u_0 e^{a't}$, a' being a constant and the plate temperature is raised to T_w . A uniform magnetic field B_0 is applied perpendicular to the plate. The governing equations have been solved numerically using Crank- Nicolson's method. It is found that the fluid velocity u decreases with an increase in either magnetic parameter M^2 or radiation parameter Ra . It is observed that the fluid velocity u increases with an increase in either magnetic parameter M^2 or Eckert number Ec . It is also found that the fluid temperature θ decreases with an increase in radiation parameter Ra . Further, it is found that the absolute value of the shear stress τ_x at the plate ($\eta = 0$) increases with an increase in either Ra or M^2 or Ec . The rate of heat transfer $-\left(\frac{d\theta}{d\eta}\right)_{\eta=0}$ at the plate ($\eta = 0$) decreases with an increase in Ra .

II. FORMULATION OF THE PROBLEM AND ITS SOLUTION

Consider the unsteady hydrodynamic flow of a viscous incompressible radiative fluid past an exponentially accelerated vertical plate in the presence of a uniform transverse magnetic field on taking into account viscous and Joule dissipations. The x -axis is taken along the vertical plate in an upward direction and y -axis is taken normal to the plate (see Fig.1). At time $t \leq 0$, both the fluid and plate are at rest with constant temperature T_∞ . At time $t > 0$, the plate at $y = 0$ starts to move in its own plane with a velocity $u_0 e^{a't}$, a' being a constant and T_w is the plate temperature. A uniform magnetic field B_0 is applied perpendicular to the plate. It is also assumed that the radiative heat flux in the x -direction is negligible as compared to that in

the y -direction. As the plate are infinite long, the velocity and temperature distribution are functions of y and t only. We assume that the magnetic Reynolds number is much less than unity and hence the induced magnetic field can be neglected in comparison with the applied magnetic field in the absence of any input electric field.

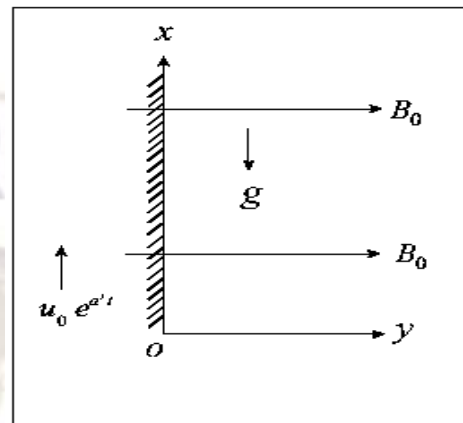


Fig.1: Geometry of the problem

Under the above assumptions and using the usual Boussinesq's approximation, the equations of momentum and energy can be written as

$$\frac{\partial u'}{\partial t} = \nu \frac{\partial^2 u'}{\partial y^2} + g\beta(T - T_\infty) - \frac{\sigma B_0^2}{\rho} u', \quad (1)$$

$$\rho c_p \frac{\partial T}{\partial t} = k \frac{\partial^2 T}{\partial y^2} + \mu \left(\frac{\partial u'}{\partial y} \right)^2 + \sigma B_0^2 u'^2 - \frac{\partial q_r}{\partial y}, \quad (2)$$

where u' is the velocity in the x -direction, T the temperature of the fluid, g the acceleration due to gravity, β the coefficient of thermal expansion, ν the kinematic coefficient of viscosity, ρ the fluid density, k the thermal conductivity, c_p the specific heat at constant pressure and q_r the radiative heat flux.

The initial and boundary conditions are $u' = 0, T = T_\infty$ for all $y \geq 0$ and $t \leq 0$,

$$u' = u_0 e^{a't}, T = T_w \text{ at } y = 0 \text{ at } t > 0, \quad (3)$$

$$u' \rightarrow 0, T \rightarrow T_\infty \text{ as } y \rightarrow \infty \text{ for } t > 0.$$

It has been shown by Cogley et al.[13] that in the optically thin limit for a non-gray gas near equilibrium, the following relation holds

$$\frac{\partial q_r}{\partial y} = 4(T - T_\infty) \int_0^\infty K_\lambda \left(\frac{\partial e_{\lambda p}}{\partial T} \right) d\lambda, \quad (4)$$

where K_λ is the absorption coefficient, λ is the wave length, $e_{\lambda p}$ is the Planck's function and subscript '0' indicates that all quantities have been

evaluated at the temperature T_∞ which is the temperature of the plate at time $t \leq 0$. Thus, our study is limited to small difference of plate temperature to the fluid temperature.

On the use of the equation (4), equation (2) becomes

$$\rho c_p \frac{\partial T}{\partial t} = k \frac{\partial^2 T}{\partial y^2} - 4(T - T_\infty)I + \mu \left(\frac{\partial u'}{\partial y} \right)^2 + \sigma B_0^2 u^2, \quad (5)$$

where

$$I = \int_0^\infty K_{\lambda_0} \left(\frac{\partial e_{\lambda p}}{\partial T} \right)_0 d\lambda. \quad (6)$$

Introducing non-dimensional variables

$$\eta = \frac{yu_0}{\nu}, \quad \tau = \frac{tu_0^2}{\nu}, \quad u = \frac{u'}{u_0}, \quad \theta = \frac{T - T_\infty}{T_w - T_\infty}, \quad (7)$$

equations (1) and (5) become

$$\frac{\partial u}{\partial \tau} = Gr\theta + \frac{\partial^2 u}{\partial \eta^2} - M^2 u, \quad (8)$$

$$Pr \frac{\partial \theta}{\partial \tau} = \frac{\partial^2 \theta}{\partial \eta^2} + PrEc \left\{ \left(\frac{\partial u}{\partial \eta} \right)^2 + M^2 u^2 \right\} - Ra\theta, \quad (9)$$

where $M^2 = \frac{\sigma B_0^2}{\rho u^2}$ is the magnetic parameter,

$Ra = \frac{4IT_\infty}{k}$ the radiation parameter, $Pr = \frac{\rho \nu c_p}{k}$ the

Prandtl number, $Gr = \frac{g \beta \nu (T_w - T_\infty)}{u_0^3}$ the Grashof

number and $Ec = \frac{u_0^2}{c_p (T_w - T_\infty)}$ the Eckert number.

The corresponding boundary conditions for u and θ are

$$\begin{aligned} u = 0, \theta = 0 \text{ for } \eta \geq 0 \text{ and } \tau \leq 0, \\ u = e^{a\tau}, \theta = 1 \text{ at } \eta = 0 \text{ for } \tau > 0, \\ u \rightarrow 0, \theta \rightarrow 0 \text{ as } \eta \rightarrow \infty \text{ for } \tau > 0, \end{aligned} \quad (10)$$

where $a = \frac{\nu a'}{u_0^2}$ is the accelerated parameter.

III. NUMERICAL SOLUTION

One of the most commonly used numerical methods is the finite difference technique, which has better stability characteristics, and is relatively simple, accurate and efficient. Another essential feature of this technique is that it is based on an iterative procedure and a tridiagonal matrix manipulation. This method provides satisfactory results but it may fail when applied to problems in which the differential equations are very sensitive to the choice

of initial conditions. In all numerical solutions the continuous partial differential equation is replaced with a discrete approximation. In this context the word *discrete* means that the numerical solution is known only at a finite number of points in the physical domain. The number of those points can be selected by the user of the numerical method. In general, increasing the number of points not only increases the resolution but also the accuracy of the numerical solution. The discrete approximation results in a set of algebraic equations that are evaluated (or solved) for the values of the discrete unknowns. The mesh is the set of locations where the discrete solution is computed. These points are called nodes and if one were to draw lines between adjacent nodes in the domain the resulting image would resemble a net or mesh.

When time dependent solutions are important, the Crank-Nicolson scheme has significant advantages. The Crank-Nicolson scheme is not significantly more difficult to implement and it has a temporal truncation error that is $O(\Delta \tau^2)$ as explained by Recktenwald [14]. The Crank-Nicolson scheme is implicit, it is also unconditionally stable [15- 17]. In order to solve the equations (8) and (9) under the initial and boundary conditions (10), an implicit finite difference scheme of Crank-Nicolson's type has been employed. The right hand side of the equations (8) and (9) is approximated with the average of the central difference scheme evaluated at the current and the previous time step. The finite difference equation corresponding to equations (8) and (9) are as follows:

$$\begin{aligned} & \frac{u_{i,j+1} - u_{i,j}}{\Delta \tau} \\ & = \left(\frac{u_{i-1,j} - 2u_{i,j} + u_{i+1,j} + u_{i-1,j+1} - 2u_{i,j+1} + u_{i+1,j+1}}{2(\Delta \eta)^2} \right) \\ & + \frac{Gr}{2} (\theta_{i,j+1} + \theta_{i,j}) - \frac{M^2}{2} (u_{i,j+1} + u_{i,j}), \end{aligned} \quad (11)$$

$$\begin{aligned} & Pr \frac{\theta_{i,j+1} - \theta_{i,j}}{\Delta \tau} \\ & = \left(\frac{\theta_{i-1,j} - 2\theta_{i,j} + \theta_{i+1,j} + \theta_{i-1,j+1} - 2\theta_{i,j+1} + \theta_{i+1,j+1}}{2(\Delta \eta)^2} \right) \end{aligned}$$

$$+ PrEc \left\{ \left(\frac{u_{i+1,j} - u_{i,j}}{\Delta \eta} \right)^2 + M^2 u_{i,j} \right\} - \frac{R}{2} (\theta_{i,j+1} + \theta_{i,j}), \quad (12)$$

The boundary conditions (10) become

$$\begin{aligned} u_{i,0} = 0, \theta_{i,0} = 0 \text{ for all } i \neq 0, \\ u_{0,j} = e^{a j \Delta \tau}, \theta_{0,j} = 1, \\ u_{N,j} = 0, \theta_{N,j} = 0, \end{aligned} \quad (13)$$

where N corresponds to ∞ . Here the suffix i corresponds to y and j corresponds to τ . Also $\Delta\tau = \tau_{j+1} - \tau_j$ and $\Delta\eta = \eta_{i+1} - \eta_i$. Knowing the values of θ, u at a time τ we can calculate the values at a time $\tau + \Delta\tau$ as follows. We substitute $i = 1, 2, \dots, N-1$, in equation (12) which constitute a tri-diagonal system of equations, the system can be solved by Thomas algorithm as discussed in Carnahan et al.[18]. Thus θ is known for all values of η at time τ . Then knowing the values of θ and applying the same procedure with the boundary conditions, we calculate, u from equation (11). This procedure is continued to obtain the solution till desired time τ . The Crank-Nicolson scheme has a truncation error of $O(\Delta\tau^2) + O(\Delta\eta^2)$, i.e. the temporal truncation error is significantly smaller.

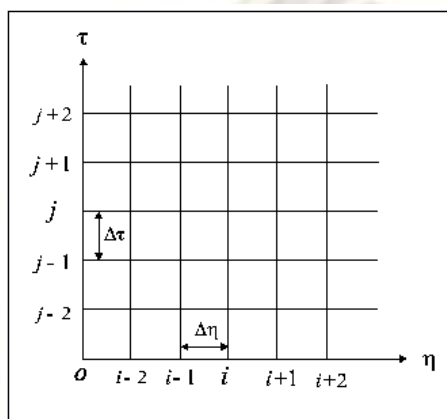


Fig.2: Finite difference grids

The implicit method gives stable solutions and requires matrix inversions which we have done at step forward in time because this problem is an initial-boundary value problem with a finite number of spatial grid points. Though, the corresponding difference equations do not automatically guarantee the convergence of the mesh $\Delta\eta \rightarrow 0$. To achieve maximum numerical efficiency, we used the tridiagonal procedure to solve the two-point conditions governing the main coupled governing equations of momentum and energy. The convergence (consistency) of the process is quite satisfactory and the numerical stability of the method is guaranteed by the implicit nature of the numerical scheme. Hence, the scheme is consistent. The stability and consistency ensure convergence.

IV. RESULTS AND DISCUSSION

We have presented the non-dimensional fluid velocity u and the fluid temperature θ for several values of the magnetic parameter M^2 , radiation parameter R , Prandtl number Pr , Grashof

number Gr , Eckert number Ec , accelerated parameter a and time τ in Figs.3-13. It is seen from Fig.3 that the velocity u decreases with an increase in magnetic parameter M^2 . This implies that the magnetic field has retarding influence on the velocity field. The presence of a magnetic field in an electrically-conducting fluid introduces a force called Lorentz force which acts against the flow if the magnetic field is applied in the normal direction as considered in the present problem. This type of resistive force tends to slow down the motion of electrically conducting fluid. It is revealed from Fig.4 that the fluid velocity u decreases with an increase in radiation parameter R . The radiation parameter arises only in the energy equation in the thermal diffusion term and via coupling of the temperature field with the buoyancy terms in the momentum equation, the velocity is indirectly influenced by thermal radiation effects. An increase in R clearly reduces the fluid velocity. Fig.5 displays that the velocity u increases with an increase in Prandtl number Pr . Fig.6 shows that the velocity u increases with an increase in Grashof number Gr . It is due to the fact that an increase of Grashof number has a tendency to increase the thermal effect. This gives rise to an increase in the induced flow. Fig.7 reveals that the fluid velocity u increases with an increase in Eckert number Ec . It is seen from Figs.8 and 9 that the velocity u increases with an increase in either accelerated parameter a or time τ . It is illustrated from Fig.10 that the fluid temperature θ increases with an increase in magnetic parameter M^2 . Fig.11 display that the fluid temperature θ decreases with an increase in radiation parameter R . This is due to the fact that the radiation provides an additional means to diffuse energy. Fig.12 shows that the fluid temperature θ increases with an increase in Prandtl number Pr . It is seen from Fig.13 that the fluid temperature θ increases with an increase in Eckert number Ec . This is due to the fact that Eckert number is the ratio of the kinetic energy of the flow to the boundary layer enthalpy difference. The effect of viscous dissipation on flow field is to increase the energy, yielding a greater fluid temperature.

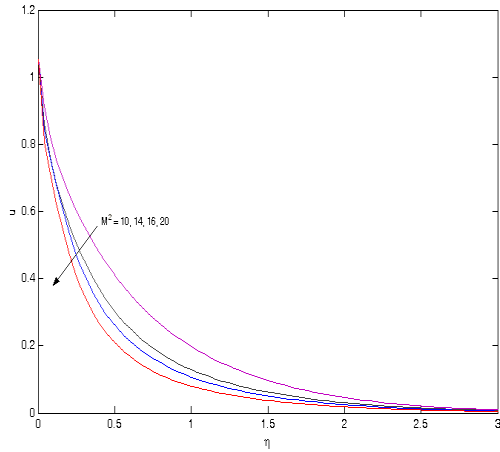


Fig.3: Velocity profiles for different M^2 when $Gr=5$, $Ra=2$, $a=0.5$, $Ec=0.5$, $Pr=0.25$ and $\tau=0.2$

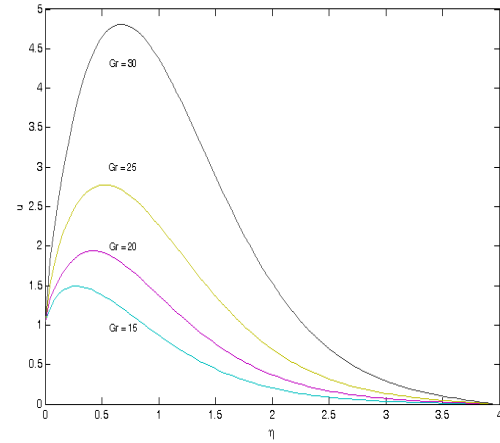


Fig.6: Velocity profiles for different Gr when $M^2=5$, $R=2$, $a=0.5$, $Ec=0.5$, $Pr=0.25$ and $\tau=0.2$

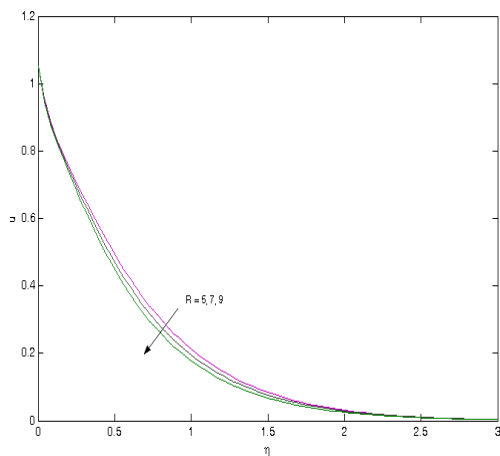


Fig.4: Velocity profiles for different R when $M^2=5$, $Gr=5$, $a=0.5$, $Ec=0.5$, $Pr=0.25$ and $\tau=0.2$

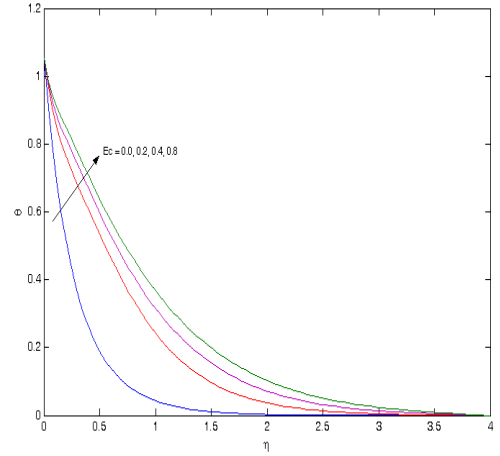


Fig.7: Velocity profiles for different Ec when $M^2=5$, $Gr=5$, $a=0.5$, $R=2$, $Pr=0.25$ and $\tau=0.2$

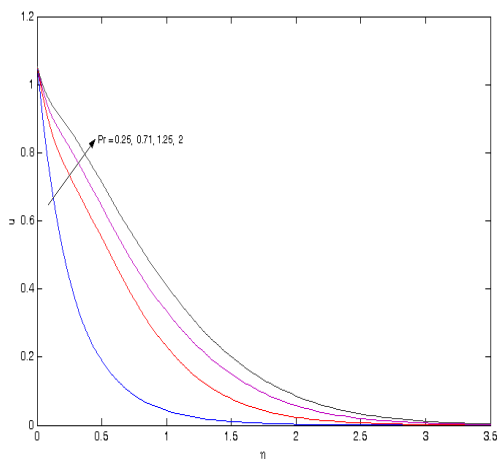


Fig.5: Velocity profiles for different Pr when $M^2=5$, $Gr=5$, $a=0.5$, $Ec=0.5$ and $\tau=0.2$

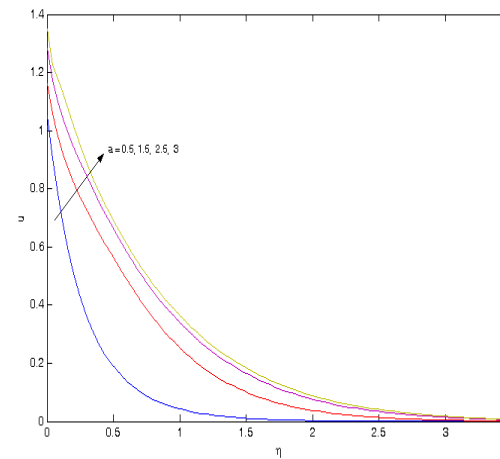


Fig.8: Velocity profiles for different a when $M^2=5$, $Gr=5$, $R=2$, $Ec=0.5$, $Pr=0.25$ and $\tau=0.2$

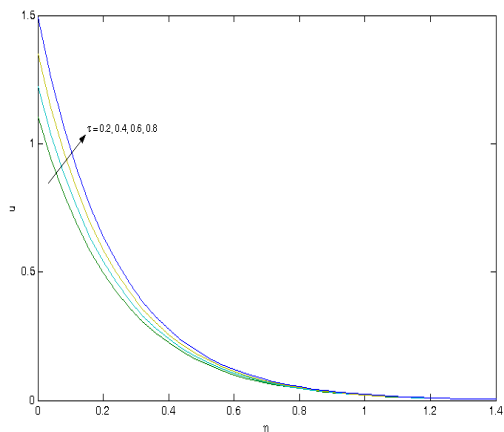


Fig.9: Velocity profiles for different time τ when $M^2 = 5$, $Gr = 5$, $a = 0.5$, $Ec = 0.5$, $Pr = 0.25$ and $R = 2$

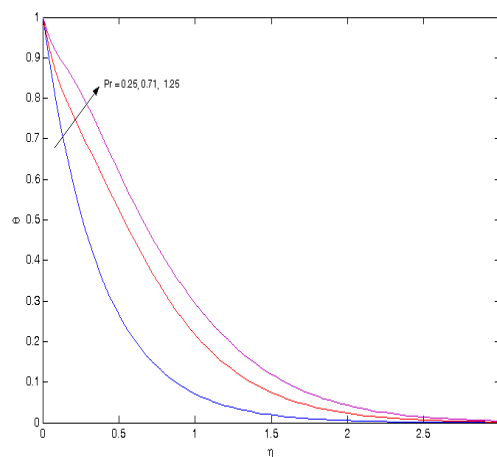


Fig.12: Temperature profiles for different Pr when $M^2 = 5$, $Ec = 0.5$, $R = 2$ and $\tau = 0.2$

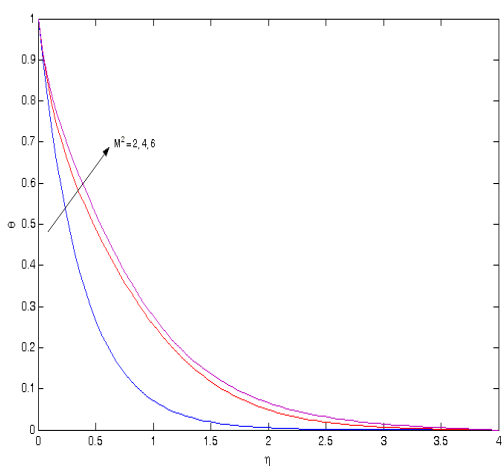


Fig.10: Temperature profiles for different M^2 when $R = 2$, $Ec = 0.5$, $Pr = 0.25$ and $\tau = 0.2$

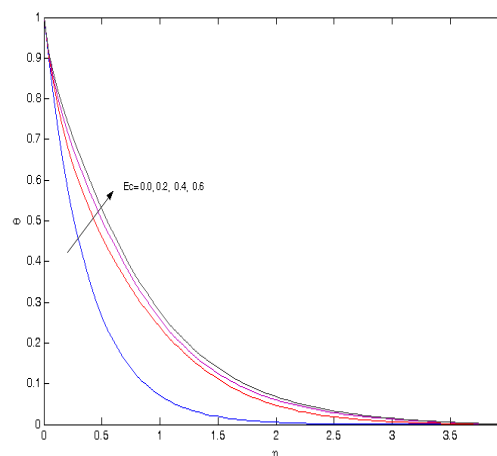


Fig.13: Temperature profiles for different Ec when $M^2 = 5$, $R = 2$, $Pr = 0.25$ and $\tau = 0.2$

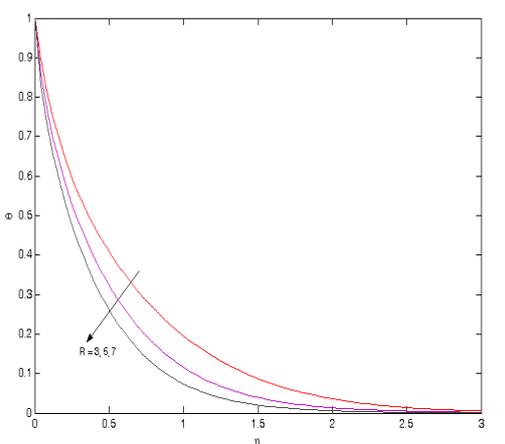


Fig.11: Temperature profiles for different R when $M^2 = 5$, $Ec = 0.5$, $Pr = 0.25$ and $\tau = 0.2$

Numerical values of the rate of heat transfer $-\theta'(0)$ at the plate $\eta = 0$ are presented in Tables 1 and 2 for several values of radiation parameter Ra , Prandtl number Pr , time τ , magnetic parameter M^2 and Eckert number Ec . It is seen from Table 1 that the rate of heat transfer $-\theta'(0)$ at the plate $\eta = 0$ decreases with an increase in either Prandtl number Pr or time τ . It is also seen that the rate of heat transfer $-\theta'(0)$ at the plate $\eta = 0$ increases with an increase in radiation parameter R . Further, it is seen from Table 2 that the rate of heat transfer $-\theta'(0)$ increases with an increase in magnetic parameter M^2 while it decreases with an increase in time τ for fixed values of radiation parameter Ra .

Table 1. Rate of heat transfer $-\theta'(0)$ at the plate $\eta = 0$

R	Pr				τ			
	0.5	0.71	1.25	1.5	0.2	0.4	0.6	0.8
2	1.45461	1.44657	1.38121	1.28118	1.40435	1.39435	1.37435	1.35435
3	1.52588	1.47031	1.34243	1.23809	1.64988	1.64132	1.63123	1.62598
4	1.64211	1.57474	1.40540	1.29520	1.71077	1.70500	1.69877	1.69085
5	1.75135	1.69003	1.51410	1.40561	1.82159	1.81524	1.80802	1.80165

Table 2. Rate of heat transfer $-\theta'(0)$ at the plate $\eta = 0$

R	M^2				Ec			
	6	8	10	12	0.1	0.2	0.3	0.4
2	1.39768	1.41948	1.43180	1.43987	1.47126	1.46680	1.45627	1.44450
3	1.60759	1.61302	1.61810	1.62216	1.66308	1.64587	1.63179	1.61808
4	1.72446	1.73223	1.73737	1.74145	1.76149	1.75448	1.74503	1.73485
5	1.81566	1.81893	1.82207	1.82467	1.84589	1.83635	1.82810	1.82001

The non-dimensional shear stress τ_x at the plate ($\eta = 0$) due to the flow is given by

$$\tau_x = \left(\frac{du}{d\eta} \right)_{\eta=0} \quad (14)$$

Numerical values of the non-dimensional shear stress τ_x due to the flow at the plate ($\eta = 0$) are presented in Figs.14-19 against radiation parameter R for several values of magnetic parameter M^2 , Grashof number Gr , Prandtl number Pr , Eckert number Ec , accelerated parameter a and time τ . Fig.14 shows that for the fixed values of the radiation parameter R , the absolute value of the shear stress τ_x increases with an increase in magnetic parameter M^2 . On other hand, it is observed that the absolute value of the shear stress τ_x decreases for $R < 1$ and it increases for $R \geq 1$ for fixed values of M^2 . Fig.15 reveals that the absolute value of the shear stress τ_x decreases for $R < 0.75$ and it increases for $R \geq 0.75$ with an increase in Prandtl number Pr . Fig.16 shows that the absolute value of the shear stress τ_x decreases with an increase in Grashof number Gr . It is illustrated from Fig.17 that the absolute value of the shear stress τ_x increases with an increase in accelerated parameter a . It is revealed from Fig.18 that the absolute value of the shear stress τ_x decreases with an increase in Eckert number Ec . Fig.19 displays that the absolute value of the shear stresses τ_x increases with an increase in time τ .

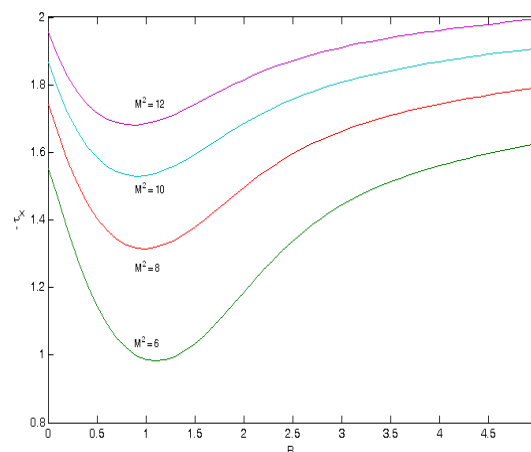


Fig.14: Shear stress τ_x for different M^2 when $Pr = 0.71$, $Gr = 5$, $a = 0.5$, $Ec = 0.5$ and $\tau = 0.2$

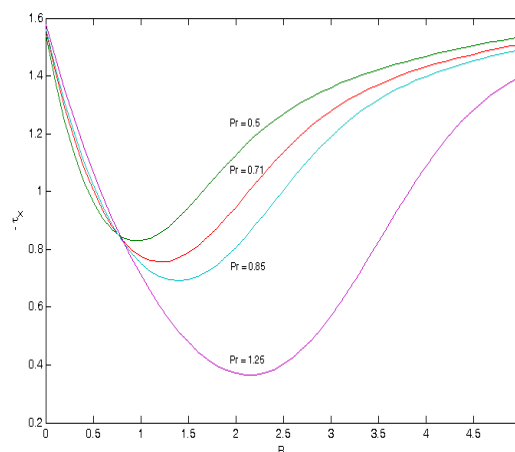


Fig.15: Shear stress τ_x for different Pr when $M^2 = 5$, $Gr = 5$, $a = 0.5$, $Ec = 0.5$ and $\tau = 0.2$

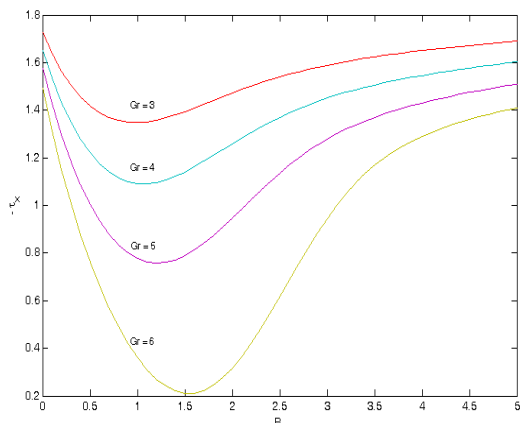


Fig.16: Shear stress τ_x for different τ when $M^2 = 5$, $Pr = 0.71$, $a = 0.5$, $Ec = 0.5$ and $\tau = 0.2$

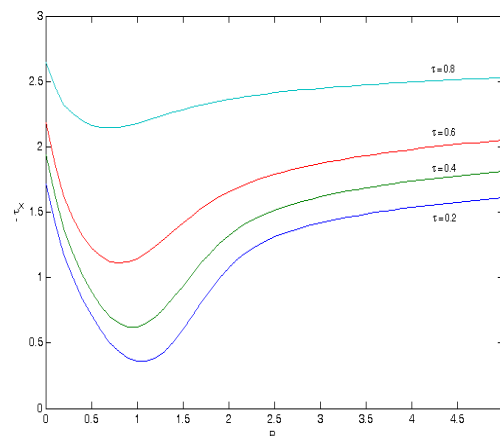


Fig.19: Shear stress τ_x for different τ when $M^2 = 5$, $Pr = 0.71$, $Gr = 5$, $a = 0.5$ and $Ec = 0.5$

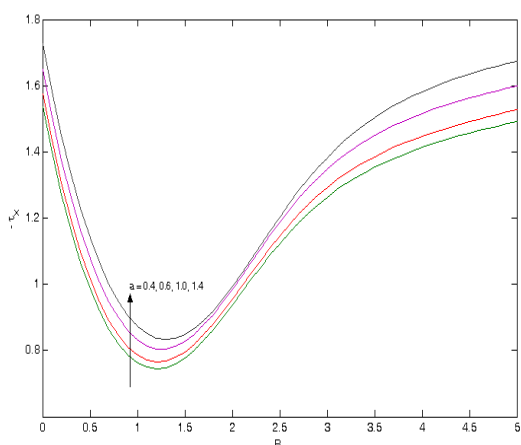


Fig.17: Shear stress τ_x for different a when $M^2 = 5$, $Pr = 0.71$, $Gr = 5$, $Ec = 0.5$ and $\tau = 0.2$

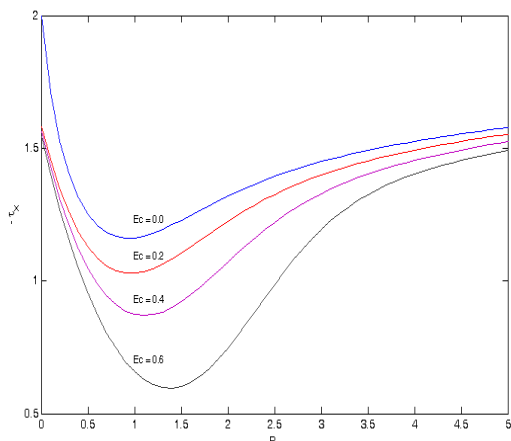


Fig.18: Shear stress τ_x for different Ec when $M^2 = 5$, $Pr = 0.71$, $Gr = 5$, $a = 0.5$ and $\tau = 0.2$

V. CONCLUSION

The radiation effects on unsteady MHD free convection flow of a viscous incompressible electrically conducting fluid past an exponentially accelerated vertical plate in the presence of a uniform transverse magnetic field by taking into account viscous and Joule dissipations have been studied. The governing equations have been solved numerically by the implicit finite difference method of Crank-Nicolson's type. It is found that the fluid velocity u decreases with an increase in either magnetic parameter M^2 or radiation parameter Ra . It is observed that the fluid velocity increases with an increase in either Grashof number Gr or time τ . It is also found that the fluid temperature θ decreases with an increase in radiation parameter Ra . Further, it is found that the absolute value of the shear stress τ_x at the plate ($\eta = 0$) increases with an increase in either Ra or M^2 or τ . The rate of heat transfer $-\theta'(0)$ at the plate ($\eta = 0$) increases with an increase in Ra or τ . It is also found that the rate of heat transfer falls with increasing Eckert number Ec .

REFERENCES

- [1] W.F. Hughes, and F. J. Young, The electro-Magneto-Dynamics of fluids, John Wiley & Sons, New York, USA (1966).
- [2] M. A. Abd-El-Naby, M.E. Elsayed, Elbarbary, Y. Nader, and Abdelzem, Finite difference solution of radiation effects on MHD free convection flow over a vertical plate with variable surface temperature. *J. Appl. Math.* 2, 2003, 65 - 86.
- [3] V. Ramachandra Prasad, N. Bhaskar Reddy, and R. Muthucumaraswamy, Transient radiative hydromagnetic free convection flow past an impulsively started vertical plate with uniform heat and mass flux. *J. App. Theo. Mech.* 33(1), 2006, 31- 63.

- [4] H.S. Takhar, R. S. R. Gorla, and V. M . Soundalgekar, Radiation effects on MHD free convection flow of a radiating fluid past a semi-infinite vertical plate. *Int. J. Numerical Methods for Heat & Fluid Flow*, 6(2), 1996, 77 - 83.
- [5] N.K. Samaria, M.U.S. Reddy, R. Prasad, H.N. Gupta, Hydromagnetic free convection laminar flow of an elasto-viscous fluid past an infinite plate, *Springer Link*, 179 (1), 2004, 39-43.
- [6] P. Sreehari Reddy, A. S. Nagarajan, M.Sivaiah, Natural convection flow of a conducting visco-elastic liquid between two heated vertical plates under the influence of transverse magnetic field, *J. Naval Archit. Marine Eng.*, 2, 2008, 47–56.
- [7] R.L. Maharajan, and B. B. Gebhart, Influence of viscous heating dissipation effects in natural convective flows, *Int. J. Heat Mass Trans.*, 32 (7), 1989, 1380–1382.
- [8] Israel – C. Cooney, A. Ogulu, and V.M. Omubo-Pepple, Influence of viscous dissipation and radiation on unsteady MHD free convection flow past an infinite heated vertical plate in a porous medium with time dependent suction, *Int. J. Heat Mass Trans.*, 46 (13), 2003, 2305-2311.
- [9] J. Zueco Jordan, Network Simulation Method Applied to Radiation and Dissipation Effects on MHD Unsteady Free Convection over Vertical Porous Plate, *Appl.Math. Modeling*, 31 (20) , 2007, 2019 – 2033.
- [10] S. Suneetha, N. Bhaskar Reddy, and V. Ramachandra Prasad, Effects of viscous dissipation and thermal radiation on hydromagnetic free convection flow past an impulsively started vertical plate, *J. Naval Archit. Marine Eng.*, 2, 2008, 57-70.
- [11] S. Suneetha, N. Bhaskar Reddy, and V. Ramachandra Prasad, Effects of thermal radiation on the natural convective heat and mass transfer of a viscous incompressible gray absorbing-emitting fluid flowing past an impulsively started moving vertical plate with viscous dissipation, *Thermal Sci.*, 13 (2), 2009, 71-181.
- [12] S. Ahmed, and A. Batin, Analytical model of MHD mixed convective radiating fluid with viscous dissipative heat, *Int. J. Engin. Sci. Tech.*, 2(9), 2010, 4902- 4911.
- [13] A.C. Cogley, W.C. Vincentine, and S.E. Gilles, A Differential approximation for radiative transfer in a non-gray gas near equilibrium, *AIAA Journal*, 6 (1968) 551-555.
- [14] G.W. Recktenwald, Finite-difference approximations to the heat equation, 2011.
- [15] W.F. Ames, Numerical Methods for Partial Differential Equations, *Academic Press, Inc., Boston*, Third edition, 1992.
- [16] E. Isaacson, and H. B. Keller, Analysis of Numerical Methods, Dover, New York, 1994.
- [17] R. L. Burden, and J. D. Faires, Numerical Analysis, *Brooks/ Cole Publishing Co.*, New York, Sixth edition, 1997.
- [18] B. Carnahan, H.A. Luther, and J.O. Wilkes, Applied Numerical Methods, John Wiley & Sons, New York (1969).